Ecosystem Health and Sustainability
A SCIENCE PARTNER JOURNAL

RESEARCH ARTICLE

Assessing Soil Carbon Components and ^{14}C to Optimize Land Use for Carbon Sequestration in the Chinese Loess Plateau

Hao Liu[1,2,3]†, Xiaocao Chen[1], Tingjun Gong[1], Xia Yu[1,2,4,5]*†, Jingfu Wang[2], Peng Cheng[4,5], and Yanling An[1]

[1]College of Resources and Environmental Engineering, Guizhou Institute of Technology, Guiyang 550003, China. [2]State Key Laboratory of Environmental Geochemistry, Institute of Geochemistry, Chinese Academy of Sciences, Guiyang 550001, China. [3]University of Chinese Academy of Sciences, College of Resources and Environment, Beijing 100049, China. [4]State Key Laboratory of Loess Science, Institute of Earth Environment, Chinese Academy of Sciences, Xi'an 710061, China. [5]Shaanxi Key Laboratory of Accelerator Mass Spectrometry Technology and Application, Xi'an 710061, China.

*Address correspondence to: yuxia@git.edu.cn
†These authors contributed equally to this work.

Citation: Liu H, Chen X, Gong T, Yu X, Wang J, Cheng P, An Y. Assessing Soil Carbon Components and ^{14}C to Optimize Land Use for Carbon Sequestration in the Chinese Loess Plateau. *Ecosyst. Health Sustain.* 2025;11:Article 0440. https://doi.org/10.34133/ehs.0440

Submitted 22 April 2025
Revised 14 October 2025
Accepted 22 October 2025
Published 27 November 2025

The Chinese Loess Plateau has approached a critical threshold in vegetation restoration, requiring optimized land-use strategies for sustainable ecosystem management. This study examines soil organic carbon (SOC) content and associated soil properties across 0 to 500 cm soil profiles under 4 land-use types (grassland, shrubland, forestland, and cropland) in the Gutun Basin. SOC dynamics were assessed using acid-soluble carbon (F1) and carbon components extracted at combustion temperatures of 25 to 400 °C (F2), 400 to 600 °C (F3), and 600 to 900 °C (F4). Based on ^{14}C ages, F1 to F3 were classified as labile components, whereas F4 was considered nonlabile. Although cropland exhibited the highest SOC stock (0.88 ± 0.38 kg m^{-2}), it also had the highest proportion of nonlabile carbon (75%). The similar ^{14}C ages of deep-soil carbon components in shrubland and forestland, along with higher carbon content in deep layers, suggested that carbon sequestration could occur at depths of at least 300 to 500 cm. However, soil water content (SWC) in shrubland and forestland was significantly lower (93.71 ± 44.94 and 71.15 ± 17.62 g kg^{-1}, respectively), and forestland exhibited lower SOC content (1.77 ± 0.56 g kg^{-1}). Among all land-use types, grassland had a significantly higher SOC content (3.96 ± 2.56 g kg^{-1}), a greater proportion of labile carbon (77%), and a higher SWC (132.06 ± 21.71 g kg^{-1}), suggesting that it was the most suitable land-use type in this context.

Introduction

In the context of global climate change and China's dual-carbon policy, research on carbon sinks has gained significant attention [1]. Soil, as the largest carbon reservoir in terrestrial ecosystems, stores approximately 4 times the carbon stock of vegetation pools and 3 times that of the atmospheric carbon pool [2]. Therefore, enhancing soil carbon sinks is a key objective in climate change mitigation research. Identifying and implementing effective methods for managing soil carbon is essential for mitigating climate change [3]. Land use significantly affects soil organic carbon (SOC) content [4,5], and scientific land management can further enhance SOC levels [6]. Research on SOC in relation to land use has predominantly focused on the top 100 cm of soil [7,8], with relatively few studies examining depths below 100 cm [9]. However, land-use types can influence the distribution of SOC in deeper soil layers via aboveground (shoot litter) and belowground (root) inputs [10], particularly for deep-rooted plant species [11]. Compared with aboveground litter, root-derived organic inputs (including root exudates) generally exhibit higher carbon conversion efficiency and contribute more substantially to the long-term stabilization of SOC [12]. In addition, subsoil carbon can rapidly accumulate on mineral surfaces that are not yet occupied by organic matter, promoting its persistence [13]. Therefore, understanding the migration, transformation, and stability of SOC in subsoil layers under different land-use types is essential for evaluating their potential to enhance deep-soil carbon stocks and support long-term carbon sequestration.

Although previous studies have examined the depth of SOC sequestration under different land-use types [14], detailed knowledge of how specific SOC fractions are distributed across soil profiles for each land-use type remains limited. Focusing solely on SOC content is insufficient for understanding its dynamics, as SOC consists of compounds with varying residence times [15]. Thus, SOC components serve as more reliable indicators of SOC quality than the content alone [16]. The ^{14}C age is useful for determining turnover times [17], providing a valuable tool for segregating distinct SOC components [18]. SOC components with older ^{14}C ages are more stable due to mineral protection and slower microbial degradation [19]. Furthermore, Hemingway et al. [20] observed that SOC components with higher activation energies and stronger mineral binding exhibit longer retention times. These findings support the method of temperature-stepped combustion to distinguish between labile and nonlabile SOC components [21]. In addition, Yu et al. [22] employed this method and found that forest nursery cropland enhances the content of labile SOC components. Incorporating the ^{14}C ages of SOC components offers valuable insights into how SOC changes with variations in soil depth.

The Chinese Loess Plateau (CLP), which covers approximately 640,000 km^2, is the world's largest loess deposit and accounts for 6.7% of China's total land area [23,24]. Considering global warming and regional characteristics, the CLP faces dual pressures from soil and water conservation and carbon sequestration efforts. The CLP is characterized by its deep, arid soils, with depths ranging from 30 to 80 cm, and in some regions, reaching several dozen meters [25]. As a result, the deep soils of the CLP offer substantial potential for increasing SOC stocks [26]. Currently, vegetation coverage in the CLP has reached a threshold of approximately 65% [27]. Consequently, optimizing the limited vegetation coverage to mitigate soil erosion and enhance carbon sequestration has become a crucial research area. This study focuses on the Gutun watershed in Yan'an City, Shaanxi Province, within the CLP. The objectives of this study were (a) to distinguish variations in labile and nonlabile SOC components across different land-use types by integrating SOC component data and ^{14}C ages, and to evaluate the carbon management levels of these land-use types; (b) to examine the carbon sequestration potential of various land-use types at different soil depths, based on variations in SOC components and ^{14}C ages; and (c) to determine the optimal vegetation type by synthesizing soil properties and carbon sequestration capacities.

Materials and Methods

Study area

The Gutun basin, covering approximately 24 km^2, is located in Baota District, Yan'an City (36°46′39″ to 37°3′34″N, 109°41′02″ to 109°56′58″E), in the central part of the CLP (Fig. 1). The average annual temperature and precipitation are 10.3 °C and 495 mm, respectively, and it belongs to a warm, subhumid climate [28]. About 70% of the rainfall occurs between June and September [29]. Additionally, the maximum annual evapotranspiration reaches 1,005 mm [30]. The watershed is located within the typical gully erosion region of the CLP, and its primary land-use types include grassland (annual plants), forestland (*Robinia pseudoacacia*), shrubland (*Sophora davidii*), and cropland.

Sample collection and analyses

Sampling

Soil samples were collected from grassland, shrubland, and forestland on hilltops, as well as from cropland in a gully, which had been cultivated with corn for 70 years. Samples were collected from large, homogeneous areas of flat land to ensure representativeness. In March and April of 2017, 1 m × 1 m quadrants were established for sampling in each land-use type. Before sampling, surface litter was removed. Soil was excavated

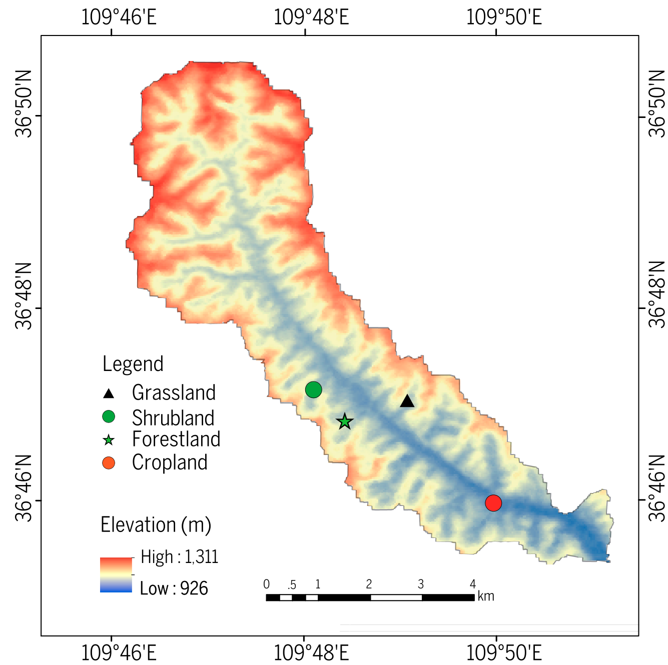

Fig. 1. Study area and sampling sites.

to a depth of 500 cm at each sampling site, or until the calcified layer was encountered. Soils were sampled in 10-cm increments from 0 to 20 cm and in 20-cm increments from 20 to 500 cm depth using 100 cm^3 ring knives and polyethylene bags. Bulk density (BD), particle size distribution, soil water content (SWC), and SOC content were determined for all sampled depths. Additionally, SOC components were analyzed at 7 selected depths: 0 to 10 cm, 20 to 40 cm, 80 to 100 cm, 180 to 200 cm, 280 to 300 cm, 380 to 400 cm, and 480 to 500 cm. The ^{14}C analysis was conducted at 3 selected depths: 0 to 10 cm, 280 to 300 cm, and 480 to 500 cm.

Soil properties and SOC determination

Soil samples were dried at 105 °C until constant weight was achieved [25], and SWC was calculated from the weight loss before and after drying. Particle size was measured using a Mastersizer 3000 laser diffractometer (Malvern Instruments, UK), and carbon content was determined using an elemental analyzer. The inorganic carbon content of the soil samples was determined by measuring the CO_2 released when carbonate was dissolved in phosphoric acid. SOC concentration was determined by subtracting inorganic carbon from bulk carbon. SOC stocks were calculated based on SOC content, BD, and soil depth.

Separation of SOC components

Soil samples were subjected to preliminary tests before temperature-stepped combustion. Three profiles were randomly selected from this area, with soil samples from depths of 0 to 10 cm, 280 to 300 cm, and 480 to 500 cm selected for combustion analysis across different temperature ranges. Approximately 10 g of the sample was reacted with phosphoric acid to obtain the F1, followed by the extraction of additional carbon components using temperature-stepped combustion. CO_2 was collected and quantified using a vacuum system. Ultimately, the temperature ranges considered suitable for the study were determined to be 25 to 400 °C (F2), 400 to 600 °C (F3), and 600 to 900 °C (F4), respectively. A detailed description of these measurements and analyses can be found in Yu et al. [22].

Determination of ^{14}C ages

The SOC was collected as CO_2 after oxidation in a vacuum system. The CO_2 was subsequently converted into graphite in a redox device, utilizing ZnO and Fe catalysts at temperatures of 425 and 575 °C [31], respectively. The resulting graphite was then compressed into an aluminum target and analyzed with a 3MV accelerator mass spectrometer (AMS) at the Xi'an AMS Center. The measurement uncertainty ($^{14}C/^{12}C$) is less than 0.3% [22].

Calculation of carbon management index

The carbon management index (CMI) is a model used to assess soil quality by comparing the soil quality of a given land to that of a reference land. Grassland was selected as the reference land due to its minimal exposure to anthropogenic disturbances in recent years.

$$CMI = CPI \times LI \times 100 \quad (1)$$

The carbon pool index (CPI) is defined as the ratio of the total carbon content in the sample (C_T sample) to that in the reference (C_T reference). The lability index (LI) represents the labile carbon content for a specific land-use type, while L denotes carbon lability (C_L: labile carbon and C_{NL}: nonlabile carbon) [32]. The sensitivity index (SI) refers to the responsiveness of the soil carbon pool to environmental changes [33].

$$CPI = C_{T\ sample} / C_{T\ reference} \quad (2)$$

$$LI = L_{sample} / L_{reference} \quad (3)$$

$$L = C_L / C_{NL} \quad (4)$$

$$SI = \left(C_{reference} - C_{sample}\right) \times 100 / C_{reference} \quad (5)$$

Statistical analysis

All data were preprocessed and organized with Excel 2019. Analysis of variance was applied to evaluate the differences in SOC across different land-use types, with a significance level set at 0.05. Pearson's correlation coefficient was employed to assess the relationships between variables, with significance levels set at 0.01 (**) and 0.05 (*) for the correlation coefficients. Statistical analysis and plotting were performed using Origin 2019b, SPSS 22, and Sigmaplot 12.5.

Results

Soil properties

BD followed the order: cropland (1.62 ± 0.16 g cm^{-3}) > shrubland (1.32 ± 0.09 g cm^{-3}) > forestland (1.29 ± 0.04 g cm^{-3}) > grassland (1.24 ± 0.07 g cm^{-3}), with cropland exhibiting significantly higher BD than the other land-use types (Table 1; $P < 0.05$). Along the 0 to 500 cm profile, BD increased with depth in all land-use types except forestland, where BD was slightly higher in the surface layer (Fig. 2). SWC followed the order: cropland (182.75 ± 25.79 g kg^{-1}) > grassland (120.44 ± 17.45 g kg^{-1}) > shrubland (93.71 ± 44.94 g kg^{-1}) > forestland (71.15 ± 17.62 g kg^{-1}), with cropland exhibiting significantly higher SWC than the other land types, and forestland showing the lowest SWC (Table 1; $P < 0.05$).

SWC below 120 g kg^{-1} is considered indicative of a dry soil layer [34]. Along the 0 to 500 cm profile, cropland had the highest proportion (95%) of SWC measurements exceeding 120 g kg^{-1}, compared to only 4% in forestland (Fig. 2), indicating that most of the forestland profile constitutes a dry soil layer. All 4 land-use types exhibited the following particle size distribution: silt (18.48% to 21.71%) > sand (75.81% to 78.03%) > clay (2.48% to 3.48%), with the clay content in cropland being significantly higher than in the other land types, while no marked differences were observed in the silt and sand content across the 4 land types (Table 1). Along the vertical profile, significant fluctuations in silt and sand content were observed in cropland (Fig. 2).

SOC characteristics

SOC content ranked from highest to lowest as follows: grassland (3.96 ± 2.56 g kg^{-1}) > cropland (2.91 ± 1.15 g kg^{-1}) > shrubland (2.76 ± 1.75 g kg^{-1}) > forestland (1.77 ± 0.56 g kg^{-1}), with grassland exhibiting significantly higher SOC than the other land-use types (Table 1; $P < 0.05$). In the vertical profile, SOC in grassland decreased with increasing soil depth and exhibited a highly significant negative correlation with soil depth ($P < 0.01$) (Fig. 3). In shrubland and cropland, SOC generally increased with depth, albeit with marked fluctuations. In contrast, no clear vertical trend was observed in forestland.

The average SOC stock ranked from highest to lowest as follows: cropland (0.88 ± 0.38 kg m^{-2}) > grassland (0.86±0.37 kg m^{-2}) > shrubland (0.69 ± 0.46 kg m^{-2}) > forestland (0.43 ± 0.13 kg m^{-2})

Table 1. Distribution characteristics of SOC and soil properties across different land-use types. Lowercase letters denote significant differences between different land-use types ($P < 0.05$).

Land-use types	BD (g cm^{-3})	SWC (g kg^{-1})	Soil texture (%)			SOC (g kg^{-1})	SOCS (kg m^{-2})
			Clay	Silt	Sand		
Grassland	1.24 ± 0.07c	132.06 ± 21.71b	2.57 ± 0.29b	76.12 ± 3.20a	21.31 ± 3.34a	3.96 ± 2.56a	0.86 ± 0.37a
Shrubland	1.32 ± 0.09b	93.71 ± 44.94c	2.68 ± 0.41b	77.63 ± 2.80a	19.70 ± 2.99a	2.76 ± 1.75ab	0.69 ± 0.46ab
Forestland	1.29 ± 0.04bc	71.15 ± 17.62d	2.48 ± 0.28b	75.81 ± 4.39a	21.71 ± 4.61a	1.77 ± 0.56b	0.43 ± 0.13b
Cropland	1.62 ± 0.16a	182.75 ± 25.79a	3.48 ± 0.93a	78.03 ± 6.31a	18.48 ± 6.95a	2.91 ± 1.15ab	0.88 ± 0.38a

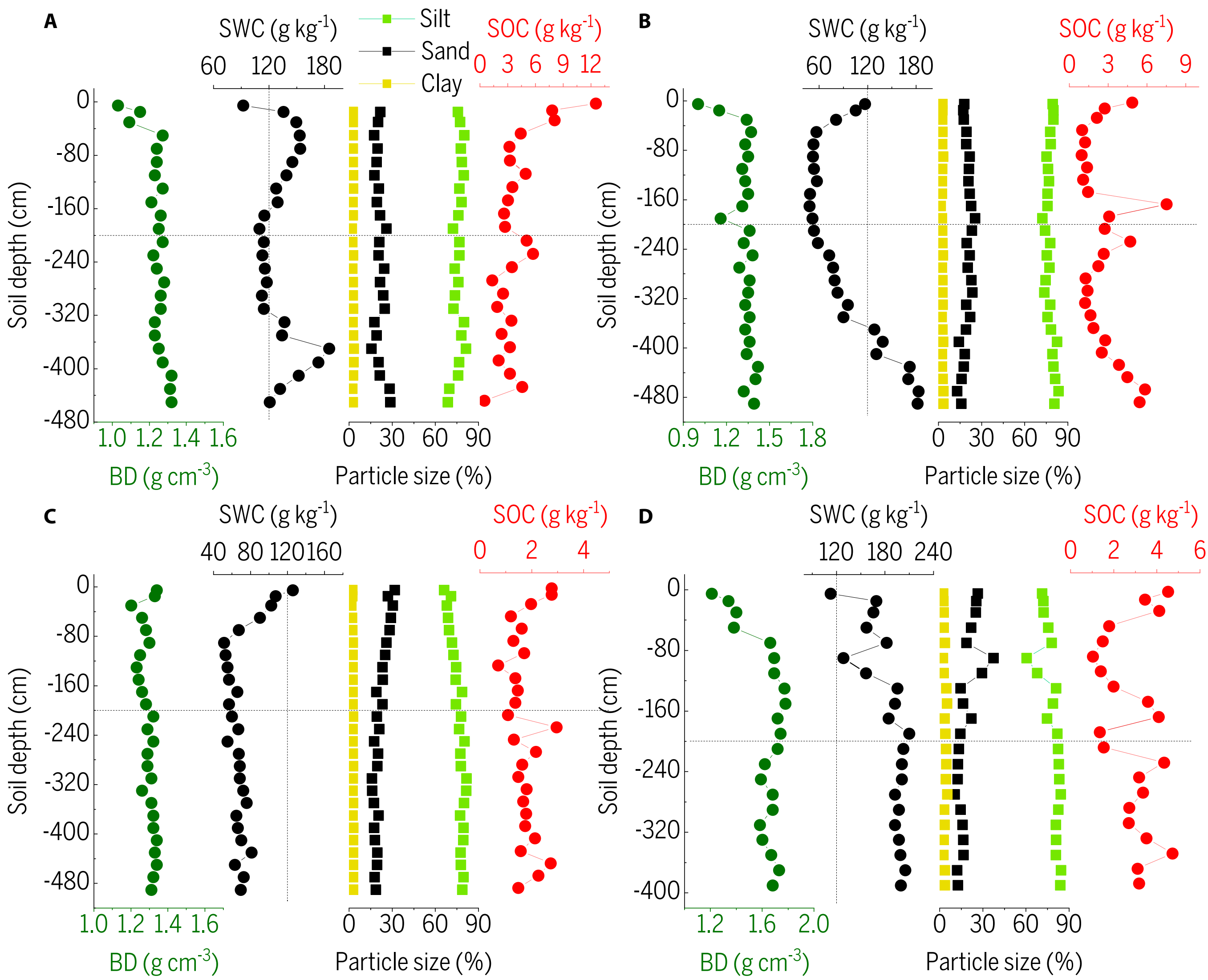

Fig. 2. Vertical distribution of soil properties and SOC. (A) Grassland, (B) shrubland, (C) forestland, and (D) cropland.

(Table 1). Except for grassland, where SOC stocks showed an extremely significant negative correlation with soil depth ($P < 0.01$), SOC stocks in the other land types exhibited a significant positive correlation with soil depth (Fig. 3; $P < 0.05$).

SOC components

F1 consistently had the lowest content among SOC components across all land-use types. However, in grassland, its concentration was not significantly different from some other components ($P > 0.05$). The dominant SOC component, in contrast, varied by land use (Table 2). Furthermore, F1 showed the lowest SI values across all land-use types (Table 2). In grassland, F3 showed the highest content (1.85 ± 1.58 g kg^{-1}), with only slight differences compared to the other components (Table 2). Similarly, in shrubland, F3 also exhibited the highest content (1.18 ± 0.97 g kg^{-1}), with only minor differences observed compared to F2 and F4, but significantly higher than F1 (Table 2; $P < 0.05$). In forestland, F2 was dominant (0.82 ± 0.37 g kg^{-1}), while in cropland, F4 exhibited the highest content (1.80 ± 0.68 g kg^{-1}), both significantly exceeding the other SOC components (Table 2; $P < 0.05$).

SOC stocks in the 0 to 500 cm soil profile were ranked as follows: shrubland (22.63 kg m^{-2}) > grassland (19.81 kg m^{-2}) > cropland (16.51 kg m^{-2}) > forestland (10.12 kg m^{-2}) (Fig. 4). The carbon components contributing the most to SOC stocks in grassland, shrubland, forestland, and cropland were F3 (38%), F3 (36%), F2 (29%), and F4 (75%), respectively (Fig. 4). Vertically, all 4 carbon components in grassland decreased with depth, with the decline becoming more pronounced in the 0 to 200 cm soil layer (Fig. 5A). In shrubland, all 4 carbon components declined in the surface layer; however, F4 increased between 200 and 300 cm, while F2 and F3 showed marked increases below 300 cm (Fig. 5B). In forestland, F2 and F3 exhibited notable changes, decreasing in the surface layer with depth, whereas F3 showed an increasing trend below 100 cm (Fig. 5C). In cropland, F2, F3, and F4 decreased markedly between 0 and 100 cm, while F4 increased below 200 cm (Fig. 5D).

According to Yu et al. [22], F1, F2, and F3 are classified as labile (active) carbon components, whereas F4 is considered a nonlabile (stable) carbon component. Consequently, the content of active SOC is ranked as follows: grassland

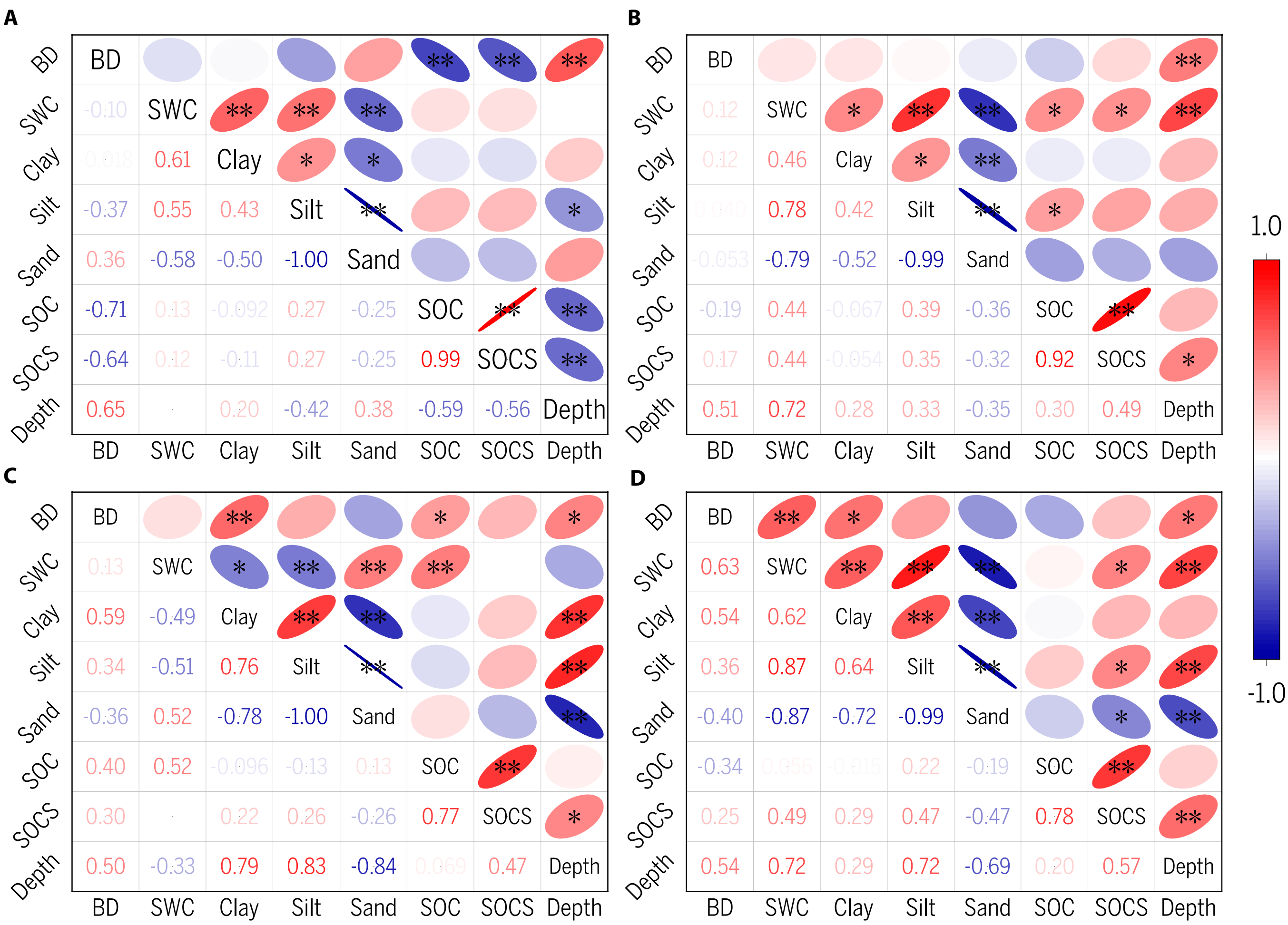

Fig. 3. Relationship among different factors. (A) Grassland, (B) shrubland, (C) forestland, and (D) cropland. In addition, SOC and SOCS represent SOC content and stocks, respectively. *$P < 0.05$; **$P < 0.01$.

Table 2. The content of SOC components across different land-use types. Uppercase letters denote differences between components of SOC, while lowercase letters denote differences between land-use types ($P < 0.05$).

Land-use types	F1 (g kg^{-1})	F2 (g kg^{-1})	F3 (g kg^{-1})	F4 (g kg^{-1})
Grassland	0.55 ± 0.48Aa	1.20 ± 1.12Aa	1.85 ± 1.58Aa	1.07 ± 1.09Ab
Shrubland	0.23 ± 0.11Bb	0.84 ± 0.65ABb	1.18 ± 0.97Ab	0.68 ± 0.50ABbc
Forestland	0.11 ± 0.06Cbc	0.82 ± 0.37Ab	0.48 ± 0.17Bc	0.31 ± 0.11BCc
Cropland	0.02 ± 0.02Bc	0.47 ± 0.51Bc	0.54 ± 0.54Bc	1.80 ± 0.68Aa

(3.60 g kg^{-1}) > shrubland (2.24 g kg^{-1}) > forestland (1.42 g kg^{-1}) > cropland (1.02 g kg^{-1}) (Table 3). Except for cropland, the proportion of labile organic carbon exceeded that of stable organic carbon in all other land-use types (Fig. 4). The L values were ranked as follows: forestland (4.58) > grassland (3.36) > shrubland (3.29) > cropland (0.57), with the L values of grassland, forestland, and shrubland being 5.89, 5.77, and 8.04 times greater than that of cropland, respectively (Table 3). Moreover, cropland exhibited the lowest LI (0.17) and CMI (10.19), whereas forestland had the lowest CPI (0.37) (Table 3).

The ^{14}C ages of SOC

The ^{14}C ages of SOC across land-use types were in the order: cropland (24,629 years) > shrubland (14,961 years) > forestland (13,559 years) > grassland (10,446 years) (Fig. 6). Among SOC components, F4 consistently had the oldest ^{14}C age, whereas the youngest component varies by land-use type: F2 in grassland (10,472 years), F3 in shrubland (13,674 years), F1 in forestland (12,909 years), and F2 in cropland (5,168 years) (Fig. 6). In surface soils, the ^{14}C ages of grassland F1, F2, and F3, as well as forestland F1, were undetectable, and the ^{14}C age of grassland F4 was only 945 years (Fig. 6A and C). Moreover, the difference in ^{14}C ages between active and stable carbon in the surface soil layer of grassland and shrubland was smaller than that in forestland and cropland, with the stable SOC components in forestland and cropland exhibiting older ^{14}C ages (Fig. 6). In deeper soil layers, the ^{14}C ages of SOC components in grassland and cropland were more widely dispersed than those in shrubland and forestland (Fig. 6).

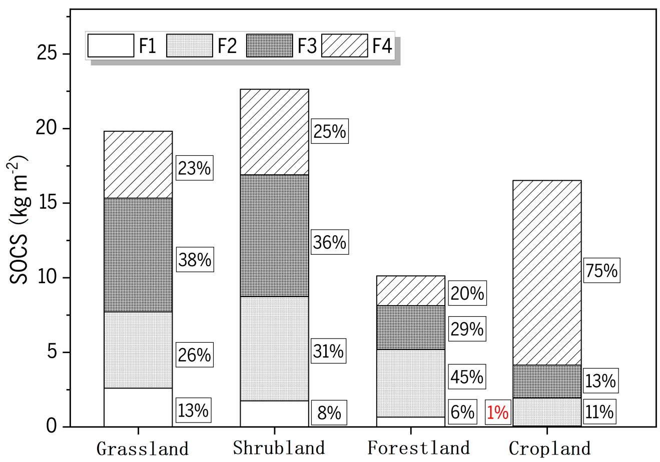

Fig. 4. Cumulative SOC component stocks in the 0 to 500 cm soil profile. The 1% marked in red represents the proportion of F1.

Discussion

Evaluation of soil carbon stock levels

Distinct differences in soil carbon cycling and pool functions were observed among the various land-use types in the study area. Grassland and shrubland exhibited higher CMI values (Table 3), primarily due to a more balanced ratio between labile and nonlabile carbon components. This balance reflected enhanced SOC stability and greater carbon cycling efficiency. Extensive root systems in grassland and abundant litter inputs in shrubland improved soil structure and promoted aggregate formation, thereby reducing the BD [35]. This lower density indicates a looser, more porous soil structure that facilitates root proliferation, water infiltration, aeration, and microbial activity [36]. The F1 component, representing the most sensitive carbon pool (Table 4), was more abundant in grassland and shrubland than in forestland or cropland, providing ample substrates for microbial metabolism. Combined with favorable soil porosity and aeration, this enrichment of labile carbon supported active microbial communities, accelerated nutrient cycling, and enhanced the transformation and stabilization of organic matter.

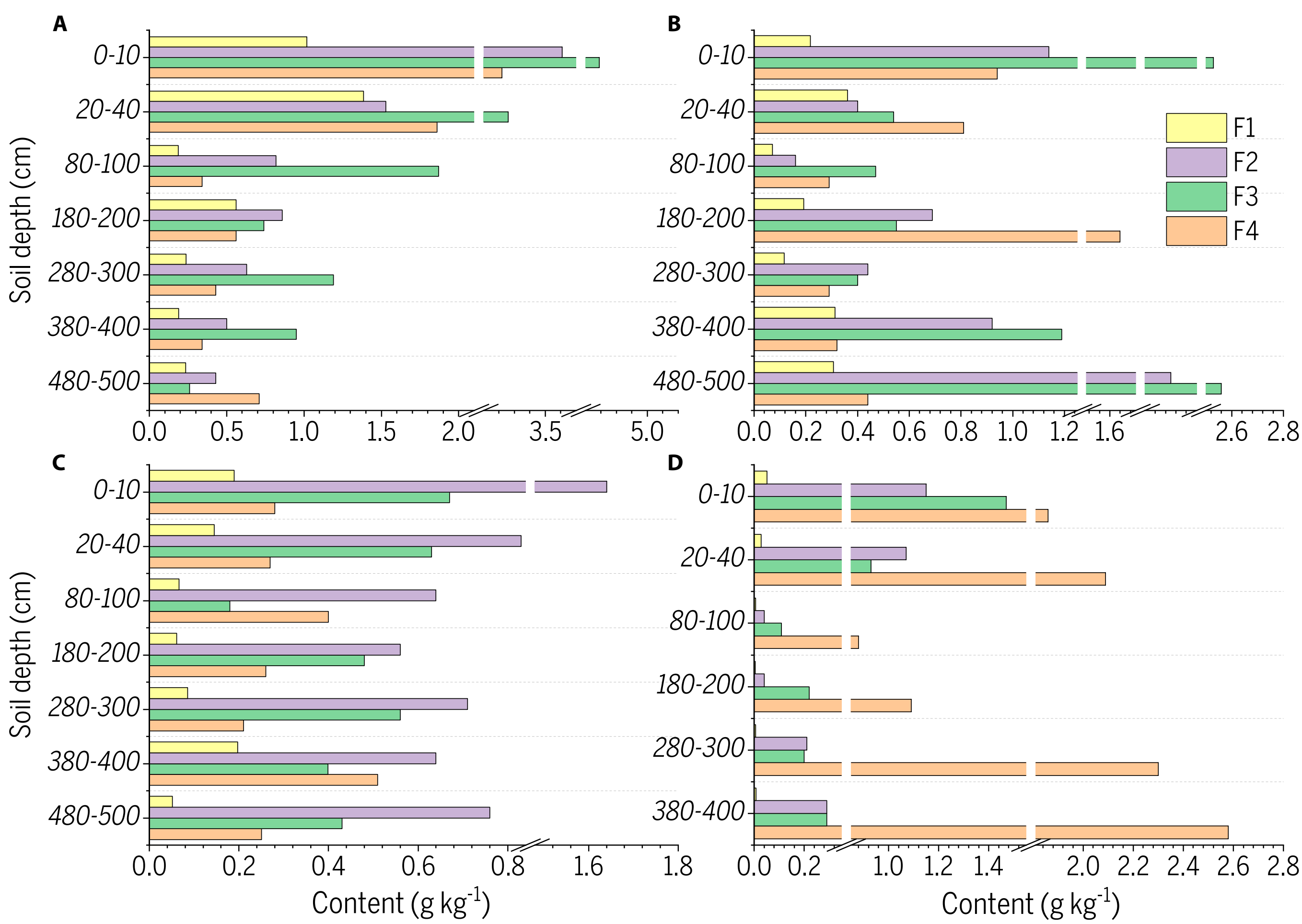

Fig. 5. Vertical distribution of SOC components content. (A) Grassland, (B) shrubland, (C) forestland, and (D) cropland.

Table 3. CMI across different land-use types. For shrubland, forestland, and cropland, LI and CPI are calculated relative to grassland, based on the ratios of L and TOC, respectively.

Land-use types	Labile SOC (g kg^{-1})	Non-labile SOC (g kg^{-1})	TOC (g kg^{-1})	L	LI	CPI	CMI
Grassland	3.60	1.06	4.66	3.36	1	1	100
Shrubland	2.24	0.68	2.92	3.29	0.98	0.63	61.22
Forestland	1.42	0.31	1.73	4.58	1.36	0.37	50.44
Cropland	1.02	1.80	2.82	0.57	0.17	0.60	10.17

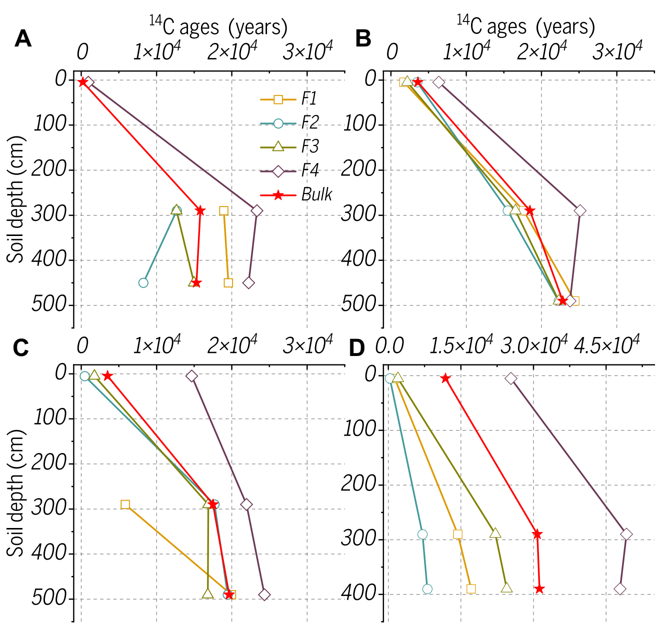

Fig. 6. The ^{14}C ages of SOC and its components. (A) Grassland, (B) shrubland, (C) forestland, and (D) cropland.

Table 4. SI of the soil carbon pool across different land-use types

Land-use types	F1	F2	F3	F4	SOC
Grassland	—	—	—	—	—
Shrubland	58	30	36	36	37
Forestland	80	32	74	71	63
Cropland	96	61	71	-68	39

In contrast, cropland and forestland displayed lower CMI values, likely resulting from anthropogenic disturbances and environmental constraints, respectively. Cropland exhibited the lowest CMI and relatively high BD due to mechanical compaction and organic matter depletion, leading to structural degradation [37]. Such compaction restricts gas exchange and microbial activity, thereby suppressing organic matter decomposition and promoting the persistence of stable or older SOC components, as evidenced by the higher proportion of F4 in cropland (Fig. 4). Although these components contribute to long-term carbon retention, they limit the continuous accumulation of SOC and the improvement of soil fertility. Forestland was primarily constrained by low SWC, a result of high transpiration rates, hydrophobic litter, and poor water-holding capacity. These conditions suppressed microbial decomposition and reduced primary productivity, thereby decreasing carbon inputs [38]. Despite a relatively high proportion of labile carbon, water limitation constrained overall SOC accumulation. Marked differences in ^{14}C ages among SOC components in cropland and forestland further indicated discontinuous and weakly dynamic carbon cycling. Overall, grassland and shrubland maintain the highest-quality SOC pools, combining strong sequestration capacity with structural stability, whereas cropland and forestland are constrained by human disturbance and soil moisture deficits, respectively.

Impact on soil carbon sequestration depth

Distinct variations in the vertical distribution of SOC were observed among the different land-use types, revealing contrasts in sequestration depth and controlling mechanisms. In grassland, SOC content declined sharply with depth (Fig. 5A), indicating that carbon inputs were largely confined to surface horizons. In contrast, shrubland, forestland, and cropland exhibited positive relationships between SOC and soil depth (Fig. 3), although the underlying processes differed among them. The most pronounced positive trend occurred in shrubland (Fig. 3C), where increasing F2 and F3 component contents with depth indicated that deep-rooted vegetation actively transported carbon downward through root exudation and turnover, forming a continuous carbon pathway from the surface to the subsoil. Forestland showed a relatively uniform SOC distribution throughout the profile, reflecting balanced root allocation and the leaching of dissolved organic matter. However, its total carbon storage was constrained by limited soil water availability. Cropland, by comparison, displayed marked vertical heterogeneity associated with tillage and soil inversion, while the enrichment of stable F4 components in deeper layers further demonstrated the influence of agricultural management on SOC redistribution [39].

Vertical variations in ^{14}C ages among SOC components provided additional insight into carbon turnover dynamics and sequestration stability. In shrubland and forestland, ^{14}C ages remained relatively consistent throughout the profile (Fig. 6B and C), suggesting steady carbon renewal and well-integrated carbon cycling [22]. The higher proportion of labile carbon in deeper layers indicated sustained carbon inputs to subsoil horizons [40]. However, despite its vertical carbon transport capacity, forestland maintained overall low SOC levels, limiting its sequestration efficiency. In grassland and cropland, marked differences in ^{14}C ages among SOC components along the profile indicated discontinuous carbon dynamics and restricted downward transfer of the new carbon (Fig. 6A and D). In cropland, the coexistence of stable carbon accumulation and substantial ^{14}C age differences further suggested that frequent tillage accelerates surface carbon loss while promoting the persistence of older carbon in deeper layers [41]. Collectively, these findings highlight shrubland as the most effective land-use type for stable deep-soil carbon sequestration through continuous root-mediated inputs. In contrast, forestland exhibits moderate but moisture-limited potential, grassland primarily accumulates carbon in surface soils, and cropland remains strongly influenced by management practices.

Land-use type favorable for soil carbon sequestration

Beyond its carbon sequestration potential, soil water conservation must also be considered in the arid Loess Plateau, where severe erosion and water scarcity strongly constrain ecosystem functioning. Forestland exhibited a significant positive correlation between SWC and the proportion of sand (Fig. 3), likely reflecting the high water consumption of *R. pseudoacacia* [42], which reduces SWC and limits SOC accumulation [38]. In contrast, cropland exhibited relatively high SWC and SOC content; however, most of its carbon comprised stable or older components, with labile SOC accounting for only about 25% of total SOC stocks. Although this composition suggests apparent carbon retention, the low bioavailability of carbon restricts microbial activity and nutrient cycling, thereby constraining the ecological functionality of the carbon pool. Improving cultivation systems through optimized tillage practices, increased residue retention, and the application of organic amendments could enhance SOC quality and promote sustainable soil functions in cropland ecosystems.

Grassland exhibited the highest SOC content, the highest CMI values, and relatively high SWC among the examined land-use types, identifying it as the most favorable system for carbon accumulation in this region. Nevertheless, its potential for deep-soil carbon sequestration was limited, whereas shrubland could stabilize carbon at depths of 300 to 500 cm through extensive root systems. The relatively high SWC in grassland can alleviate the water deficit commonly observed in shrubland. These complementary features, together with evidence that SOC storage increases with plant diversity [43], strongly support the synergistic potential of grassland and shrubland assemblages. Such mixed systems may simultaneously enhance deep-soil carbon sequestration in grassland and improve water-use efficiency in shrubland, representing an effective strategy for optimizing carbon storage and sustaining ecosystem resilience on the Loess Plateau.

Conclusion

This study focuses on the Gutun watershed in the CLP, where temperature-stepped combustion was used to extract SOC components, combined with ^{14}C dating, to assess the SOC quality in grassland, shrubland, forestland, and cropland. The findings of this study are as follows: (a) Grassland is the most effective land-use type for water retention and carbon sequestration; (b) shrubland exhibits strong carbon sequestration potential in deeper soil layers; (c) the low SOC and SWC in forestland hinder water-carbon retention; and (d) the high proportion of inert carbon in cropland restricts both carbon sequestration and the sustainable development of agricultural lands.

Implementing mixed vegetation systems, such as combining grassland and shrubland, could be an effective strategy for enhancing water retention and carbon sequestration in the Gutun watershed. Therefore, it is recommended to further investigate the soil carbon sequestration potential and quality under the combined state of shrubland and grassland. Moreover, since this study only provided preliminary measurements of the ^{14}C ages for soil samples from the surface, middle, and deep layers, it is unable to precisely determine the carbon sequestration depth. Future studies should include more detailed ^{14}C age analyses.

Acknowledgments

Funding: This work was financially supported by the Strategic Pilot Project (Class B) of the Chinese Academy of Sciences (No. XDB4000000), the Open Fund of State Key Laboratory of Loess and Quaternary Geology (No. SKLLQG2036), the Guizhou Provincial Science and Technology Support Program (No. QianKeHeJiChu-ZK [2024] YiBan511), and the Research Initiation Program for High-level Talents of Guizhou Institute of Technology in 2023 (No. 2023GCC082).
Author contributions: H.L.: Writing—review and editing, writing—original draft, visualization, validation, and formal analysis. X.C.: Visualization and investigation. T.G.: Visualization and investigation. X.Y.: Writing—review and editing, funding acquisition, data curation, and conceptualization. J.W.: Validation and resources. P.C.: Writing—review and editing, resources, and conceptualization. Y.A.: Validation and resources.
Competing interests: The authors declare that they have no competing interests.

Data Availability

Data will be made available on request.

References

1. Yang Y, Shi Y, Sun W, Chang J, Zhu J, Chen L, Wang X, Guo Y, Hongtu Z, Yu L, et al. Terrestrial carbon sinks in China and around the world and their contribution to carbon neutrality. *Sci China Life Sci*. 2022;65(5):861–895.
2. Lal R, Monger C, Nave L, Smith P. The role of soil in regulation of climate. *Philos Trans R Soc Lond*. 2021;376(1834):20210084.
3. Amelung W, Bossio D, de Vries W, Kögel-Knabner I. Towards a global-scale soil climate mitigation strategy. *Nat Commun*. 2020;11(1):5427.
4. Laganiere J, Angers DA, Pare D. Carbon accumulation in agricultural soils after afforestation: A meta-analysis. *Glob Chang Biol*. 2010;16(1):439–453.
5. Deng L, Liu G, Shangguan Z. Land-use conversion and changing soil carbon stocks in China's grain-for-green' program: A synthesis. *GLOB Chang Biol*. 2014;20(11):3544–3556.
6. Ali S, Begum F, Hayat R, Bohannan BJ. Variation in soil organic carbon stock in different land uses and altitudes in Bagrot Valley, Northern Karakoram. *Acta Agric Scand B*. 2017;67(6):551–561.
7. Shi P, Zhang Y, Li P, Li Z, Yu K, Ren Z, Xu G, Cheng S, Wang F, Ma Y. Distribution of soil organic carbon impacted by land-use changes in a hilly watershed of the loess plateau. *China Sci Total Environ*. 2019;652:505–512.

8. Zhong Z, Han X, Xu Y, Zhang W, Fu S, Liu W, Ren C, Yang G, Ren G. Effects of land use change on organic carbon dynamics associated with soil aggregate fractions on the loess plateau. *China Land Degrad Dev*. 2019;30(9):1070–1082.
9. James J, Devine W, Harrison R, Terry T. Deep soil carbon: Quantification and modeling in subsurface layers. *Soil Sci Soc Am J*. 2014;78(S1):S1–S10.
10. Rumpel C, Kögel KI. Deep soil organic matter—A key but poorly understood component of terrestrial C cycle. *Plant Soil*. 2011;338(1–2):143–158.
11. Dou X, Deng Q, Li M, Wang W, Zhang Q, Cheng X. Reforestation of *Pinus massoniana* alters soil organic carbon and nitrogen dynamics in eroded soil in South China. *Ecol Eng*. 2013;52:154–160.
12. Villarino SH, Pinto P, Jackson RB, Piñeiro G. Plant rhizodeposition: A key factor for soil organic matter formation in stable fractions. *Sci Adv*. 2021;7(16):Article eabd3176.
13. Schiedung M, Don A, Beare MH, Abiven S. Soil carbon losses due to priming moderated by adaptation and legacy effects. *Nat Geosci*. 2023;16(10):909–914.
14. Zhou J, Wang Y, Tong Y, Sun H, Zhao Y, Zhang P. Regional spatial variability of soil organic carbon in 0–5 m depth and its dominant factors. *Catena*. 2023;231:107326.
15. Wei J, Cheng J, Li W, Liu W. Comparing the effect of naturally restored forest and grassland on carbon sequestration and its vertical distribution in the Chinese loess plateau. *PLOS ONE*. 2012;7(7):Article e40123.
16. Borges O, Raimundo F, Coutinho J, Gonçalves B, Oliveira I, Martins A, Madeira M. Carbon fractions as indicators of organic matter dynamics in chestnut orchards under different soil management practices. *Agrofor Syst*. 2018;92:301–310.
17. Trumbore S. Radiocarbon and soil carbon dynamics. *Annu Rev Earth Planet Sci*. 2009;37(1):47–66.
18. Grant KE, Galy VV, Haghipour N, Eglinton TI, Derry LA. Persistence of old soil carbon under changing climate: The role of mineral-organic matter interactions. *Chem Geol*. 2022;587:120629.
19. Gentsch N, Wild B, Mikutta R, Čapek P, Diáková K, Schrumpf M, Turner S, Minnich C, Schaarschmidt F, Shibistova O. Temperature response of permafrost soil carbon is attenuated by mineral protection. *Glob Change Biol*. 2018;24(8):3401–3415.
20. Hemingway JD, Rothman DH, Grant KE, Rosengard SZ, Eglinton TI, Derry LA, Galy VV. Mineral protection regulates long-term global preservation of natural organic carbon. *Nature*. 2019;570(7760):228–231.
21. Cheng P, Zhou W, Wang H, Lu X, Du H. ^{14}C dating of soil organic carbon (SOC) in loess-paleosol using sequential pyrolysis and accelerator mass spectrometry (AMS). *Radiocarbon*. 2013;55(2):563–570.
22. Yu X, Zhou W, Wang Y, Cheng P, Hou Y, Du H, Xiong X, Yang L, Wang Y, Fu Y. Sequential combustion separation of soil organic carbon fractions for AMS measurement of ^{14}C and their application in fixation of carbon. *J Radioanal Nucl Chem*. 2020;323(1):169–177.
23. Li X, Jin Z, Zhang X, Zhou W. Analysis of ecosystem management of the loess plateau during the past 60 years and suggestions for the future development. *Earth Environ*. 2015;6:248–254.
24. Jin Z, Li G, Lin H, Wang Y, Yu Y. Soil moisture response to rainfall on the Chinese loess plateau after a long-term vegetation rehabilitation. *Hydrol Process*. 2018;32(12):1738–1754.
25. Wang Y, Liu Z, Shao M. Vertical distribution and influencing factors of soil water content within 21-m profile on the Chinese loess plateau. *Geoderma*. 2013;193:300–310.
26. Wang S, Gao X, Yang M, Zhang L, Wang X, Wu P, Zhao X. The efficiency of organic C sequestration in deep soils is enhanced by drier climates. *Geoderma*. 2022;415:115774.
27. Chen Y, Wang K, Fu B, Wang Y, Tian H, Wang Y, Zhang Y. 65% cover is the sustainable vegetation threshold on the loess plateau. *Environ Sci Ecotechnol*. 2024;22:100442.
28. Yu Y, Henry L, Jin Z, Chu G, Zhang J. Ammonia dynamics in reservoirs in response to rainfall events in a gully-filled loess catchment in Yan'an City, Shaanxi Province. *Quat Sci*. 2017;37(6):1204–1218.
29. Li CT, Yuan Y, Wilson R. An unsupervised conditional random fields approach for clustering gene expression time series. *Bioinformatics*. 2008;24(21):2467–2473.
30. Ning T, Li Z, Liu W, Han X. Evolution of potential evapotranspiration in the northern loess plateau of China: Recent trends and climatic drivers. *Int J Climatol*. 2016;36(12):4019–4028.
31. Xiong X, Zhou W, Cheng P, Wang Y, Lu X, Du H. Preparation of graphite targets for ^{14}C dating by accelerator mass spectrometry. *J Radioanal Nucl Chem*. 2017;311(2):1283–1289.
32. Blair GJ, Lefroy RDB, Lisle L. Soil carbon fractions based on their degree of oxidation, and the development of a carbon management index for agricultural systems. *Aust J Agric Res*. 1995;46(7):1459–1466.
33. Benbi DK, Brar K, Toor AS, Singh P. Total and labile pools of soil organic carbon in cultivated and undisturbed soils in northern India. *Geoderma*. 2015;237:149–158.
34. Wang L, Shao M, Hou Q. Preliminary study on quantitative index of soil dry layer. *J Soil Water Conserv*. 2000;4:87–90.
35. Ma J, Li Z, Li P, Ma B, Xiao L, Cui Z, Wang Z, Min Z. Effect of mixed plant roots on saturated hydraulic conductivity and saturated water content of soil in the loess region. *Agric Water Manag*. 2024;295:108784.
36. Chen J, Wu Z, Zhao T, Yang H, Long Q, He Y. Rotation crop root performance and its effect on soil hydraulic properties in a clayey Utisol. *Soil Tillage Res*. 2021;213:105136.
37. Xu Y, Pei J, Li S, Zou H, Wang J. Main characteristics and utilization countermeasures for black soils in different regions of Northeast China. *Chin J Soil Sci*. 2023;54(2):495–504.
38. Yang X, Li T, Shao M. Factors controlling deep-profile soil organic carbon and water storage following *Robinia pseudoacacia* afforestation of the loess plateau in China. *For Ecosyst*. 2022;9:100079.
39. Schiedung M, Tregurtha CS, Beare MH, Thomas SM, Don A. Deep soil flipping increases carbon stocks of New Zealand grasslands. *Glob Change Biol*. 2019;25(7):2296–2309.
40. Liao C, Li D, Huang L, Yue P, Liu F, Tian Q. Higher carbon sequestration potential and stability for deep soil compared to surface soil regardless of nitrogen addition in a subtropical forest. *PeerJ*. 2020;8:Article e9128.
41. Yu X, Zhou W, Wang Y, Cheng P, Hou Y, Du H, Xiong X, Yang L, Wang Y, Fu Y. Soil organic carbon fractions and ^{14}C ages through 70 years of cropland cultivation. *Soil Tillage Res*. 2019;195:104415.
42. Fan Y, Miguez Macho G, Jobbágy EG, Jackson RB, Otero CC. Hydrologic regulation of plant rooting depth. *Proc Natl Acad Sci USA*. 2017;114(40):10572–10577.
43. Chen X, Taylor AR, Reich PB, Hisano M, Chen HY, Chang SX. Tree diversity increases decadal forest soil carbon and nitrogen accrual. *Nature*. 2023;618(7963):94–101.

Ecosystem Health and Sustainability
A SCIENCE PARTNER JOURNAL

Assessing Soil Carbon Components and 14C to Optimize Land Use for Carbon Sequestration in the Chinese Loess Plateau

Hao Liu, Xiaocao Chen, Tingjun Gong, Xia Yu, Jingfu Wang, Peng Cheng, and Yanling An

Citation: Liu H, Chen X, Gong T, Yu X, Wang J, Cheng P, An Y. Assessing Soil Carbon Components and 14C to Optimize Land Use for Carbon Sequestration in the Chinese Loess Plateau. *Ecosyst Health Sustain*. 2025;**11**:0440. DOI: 10.34133/ehs.0440

The Chinese Loess Plateau has approached a critical threshold in vegetation restoration, requiring optimized land-use strategies for sustainable ecosystem management. This study examines soil organic carbon (SOC) content and associated soil properties across 0 to 500 cm soil profiles under 4 land-use types (grassland, shrubland, forestland, and cropland) in the Gutun Basin. SOC dynamics were assessed using acid-soluble carbon (F1) and carbon components extracted at combustion temperatures of 25 to 400 °C (F2), 400 to 600 °C (F3), and 600 to 900 °C (F4). Based on 14C ages, F1 to F3 were classified as labile components, whereas F4 was considered nonlabile. Although cropland exhibited the highest SOC stock (0.88 ± 0.38 kg m#2), it also had the highest proportion of nonlabile carbon (75%). The similar 14C ages of deep-soil carbon components in shrubland and forestland, along with higher carbon content in deep layers, suggested that carbon sequestration could occur at depths of at least 300 to 500 cm. However, soil water content (SWC) in shrubland and forestland was significantly lower (93.71 ± 44.94 and 71.15 ± 17.62 g kg#1, respectively), and forestland exhibited lower SOC content (1.77 ± 0.56 g kg#1). Among all land-use types, grassland had a significantly higher SOC content (3.96 ± 2.56 g kg#1), a greater proportion of labile carbon (77%), and a higher SWC (132.06 ± 21.71 g kg#1), suggesting that it was the most suitable land-use type in this context.
Image

View the article online
https://spj.science.org/doi/10.34133/ehs.0440

Ecosystem Health and Sustainability (ISSN 2332-8878) is published by the American Association for the Advancement of Science. 1200 New York Avenue NW, Washington, DC 20005.